

# Two-photon laser scanning fluorescence microscopy using photonic crystal fiber

## Gail McConnell

University of Strathclyde  
Centre for Biophotonics  
SIBS, 27 Taylor Street  
Glasgow G4 0NR, Scotland

## Erling Riis

University of Strathclyde  
Department of Physics  
John Anderson Building  
Glasgow G4 0NG, Scotland  
E-mail: g.mcconnell@strath.ac.uk

**Abstract.** We report the application of a simple yet powerful modular pulse compression system based on photonic crystal fibers that improves on incumbent two-photon laser scanning fluorescence microscopy techniques. This system provides more than a sevenfold increase in fluorescence yield when compared with a commercial two-photon microscopy system. From this, we infer pulses of IR radiation of less than 35 fs duration reaching the sample. © 2004 Society of Photo-Optical Instrumentation Engineers. [DOI: 10.1117/1.1778734]

Keywords: multiphoton; microscopy; fluorescence; ultrafast; nonlinear.

Paper 03110 received Sep. 3, 2003; revised manuscript received Jan. 8, 2004, and Feb. 5, 2004; accepted for publication Feb. 16, 2004.

## 1 Introduction

Multiphoton laser scanning microscopy (MPLSM) is a well-established tool for deep and live imaging of biological tissue.<sup>1</sup> Two types of laser sources suited to two-photon excitation exist, namely, continuous wave (cw) and ultra-short-pulsed (USP) lasers, the latter delivering pulses typically of subpicosecond duration every few nanoseconds. The resulting peak power from USP lasers can easily reach the kilowatt level, while retaining a modest average power level. The very high peak powers generated by USP laser sources are ideal for multiphoton applications when focused using an objective lens. The primary advantage of employing an USP laser for two-photon laser scanning microscopy (TPLSM) over a cw alternative is an increase in sample viability because of the small duty cycle. This enables sample and fluorophore recovery on the nanosecond scale. An additional advantage of employing a USP source for TPLSM is the conservative average power delivered. This reduces detrimental heating effects through linear absorption that are observed when applying a cw laser source.<sup>2</sup>

The most popular choice of USP laser gain medium for TPLSM is currently Ti:sapphire. Commercial lasers based on this material can support wavelengths from 720 to 930 nm with a single mirror set, and may deliver pulses as short as 140 fs duration (e.g., the commercial products Chameleon from Coherent Inc. and Mai-Tai from Spectra Physics). The laser source is typically used in conjunction with a computer-controlled scan head that manipulates the beam profile of the entering laser, and a microscope with a high ( $>10\times$ ) magnification objective lens to focus the radiation onto the prepared biological sample for investigation and subsequent image capture. Therefore, before the laser pulse reaches the sample it is relayed by and propagated through a number of optical elements, including steering mirrors, beam-shaping optics, and filters. Unfortunately, each of these elements stretches the pulse through dispersion. As a consequence, the duration of the pulse reaching the sample is commonly much longer than that emitted by the USP laser. Efforts have been

made to precompensate for dispersion by including prisms in a home-built laser resonator, delivering pulses of 15.5 fs duration,<sup>3</sup> but this approach is inflexible when used with alternative commercial resonators.

To solve this problem, we developed an effective pulse compression technique based on photonic crystal fiber (PCF). Previous studies by Ouzounov et al.<sup>4</sup> demonstrated that ultrashort pulses can propagate through PCF, but in their investigation the emitted pulses are stretched from 100 to 140 fs. We report on a system that compresses the pulse duration and, using a conventional Ti:sapphire laser platform and standard MPLSM equipment, returns more than a sevenfold increase of the fluorescence signal (i.e., fluorescence yield) from prepared biological samples at standard excitation wavelengths. This is of particular benefit for fluorophores that are only weakly excited by standard commercially available laser units. Our modular system is an ideal accompaniment to most commercial laser sources and comprises very basic and fixed optomechanical components to facilitate ease of use.

The development<sup>5</sup> of PCF has brought renewed interest to the field of nonlinear fiber optics. PCFs are microstructured fibers, where the light is guided by a number of periodically arranged air holes that extend along the length of the fiber. These holes create a photonic bandgap in the transverse dimension, resulting, for instance, in fibers that are single-mode throughout the visible range.<sup>6</sup> Alternatively, this superior guiding property can be viewed as resulting from the large refractive index step between the fused silica core and the surrounding partly air filled cladding. This large refractive index step also enables a reduction in the core diameter to a few micrometers, leading to a significant increase in the propagating peak intensity. This is of obvious benefit in the study of nonlinear effects, but just as significant is the fact that the exact nature of the microstructure determines the group velocity dispersion (GVD) of the fiber. Typically,<sup>6</sup> the zero point  $\lambda_0$  for the GVD in a 1- to 2- $\mu\text{m}$ -diam PCF is shifted from the bulk silica value of around 1300 nm to 600 to 800 nm. This means that it is now possible to have a fiber with anomalous dispersion at a convenient wavelength, such

Address all correspondence to Gail McConnell, Centre for Biophotonics, SIBS, 27 Taylor Street, Glasgow, Scotland G4 0NR, United Kingdom. Tel: 44(141) 548 4738; FAX: 44 (141) 548 4887; E-mail: g.mcconnell@strath.ac.uk

as that of the Ti:sapphire laser. The most spectacular manifestation of this high nonlinearity in an anomalously dispersive regime is the generation of a white-light supercontinuum, which in part is due to soliton formation.<sup>7,8</sup>

The situation is far simpler for wavelengths below the zero point for the GVD. The normal dispersion prevents soliton formation, leaving self-phase modulation as the main nonlinear effect. In this paper, we investigate a dispersion precompensation scheme based on spectral broadening in a normally dispersive PCF and subsequent dispersion compensation in a grating pair. We show how the unique properties of the fiber in terms of high nonlinearity and low GVD combine to give ideal conditions for ultrashort pulse compression. The 250-fs pulses from a commercial Ti:sapphire laser are compressed to  $<35$  fs at the microscope stage. This results in more than a sevenfold increase in fluorescence detected from the biological sample. This method has significant potential for improvements through a dedicated PCF design, providing a simple and effective route to obtaining a pulse of below 10 fs duration at the sample, where laser operation is significantly more challenging.

## 2 Experiments

A schematic of the PCF-enabled laser experimental setup is shown in Fig. 1(a). A commercial Ti:sapphire laser (Coherent, Mira 900-F) emitted a 76-MHz train of pulses in the 800- to 860-nm region, with the pulse width measured to be approximately 250 fs with an interferometric autocorrelation trace consistent with a  $\text{sech}^2$  pulse shape. The same laser was used both directly and as the pump for the PCF-enabled system to directly compare performance when employed as an excitation source for TPLSM.

In the PCF-enabled system, this light was propagated through a Faraday isolator to reduce feedback from the PCF facets, which largely limited the wavelength range of operation. The output was focused into an 86-mm length of PCF using a spherical antireflection coated  $f = +4.5$  mm lens. The output was collimated and passed through a dispersion compensating stage, consisting of two parallel 600-lines/mm gratings separated by up to 16 mm. This grating pair introduced a negative dispersion in the beam of  $b_0 = 0.463 \text{ ps}^2/\text{m}$ , where  $b_0$  is the separation between the gratings.<sup>9</sup> The light transmitted by the PCF was then passed into a scan head (Bio-Rad, MRC1024ES) coupled to an inverted microscope (Nikon, TE300), as shown in Fig. 1(b). Alternatively, the conventional Ti:sapphire excitation light was similarly passed into the scan head and microscope system. The light entering the scan head was reflected and manipulated by scanning mirrors toward the microscope. A  $20\times/0.75$  NA air microscope objective lens (Nikon, Plan Fluor) was used to focus the radiation onto the fluorescently stained sample. Fluorescence resulting from two-photon excitation, using either the PCF-augmented laser or a conventional Ti:sapphire source, was collected by the same objective lens and propagated through an optical band-pass filter to reject reflected light from the excitation source. The fluorescence was then relayed to a sensitive PMT. This signal was used, along with image capture software, to visualize fluorescently stained regions of the sample.

The PCF was manufactured by Crystal Fiber A/S. It was made of pure silica and had a hexagonal structure of air holes

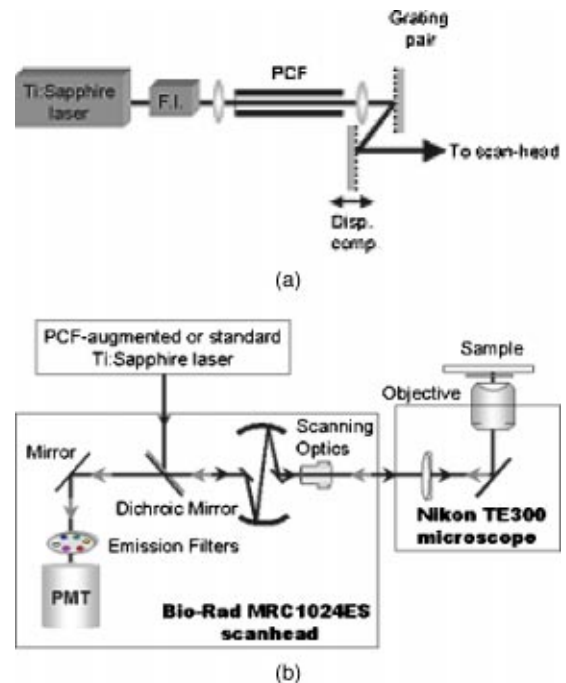


**Fig. 1** (a) Output of a mode-locked Ti:sapphire laser (Coherent Mira 900-F) is sent through a Faraday isolator (F.I.) and coupled into a section of PCF. The spectrally broadened output is compressed by the negative dispersion of a grating pair. The resultant radiation is then directed into a commercial scan head (Bio-Rad MRC 1024ES). (b) Light transmitted by either the PCF-enabled or the standard system entered into a scan head (Bio-Rad, MRC1024ES) coupled to an inverted microscope (Nikon, TE300), as shown in Fig. 1(b). Alternatively, the conventional Ti:sapphire excitation light was similarly passed into the scan head and microscope system. The light entering the scan head was reflected and manipulated by scanning mirrors toward the microscope. A  $20\times/0.75$  NA air microscope objective lens (Nikon, Plan Fluor) was used to focus the radiation onto the fluorescently stained sample. Fluorescence resulting from two-photon excitation was collected by the same objective lens and relayed to a sensitive photomultiplier tube (PMT). This signal was used, along with image capture software, to visualize fluorescently stained regions of the sample in the conventional method.

to guide the light in a  $2.6\text{-}\mu\text{m}$  core. The distance between adjacent air holes was  $1.8 \pm 0.2 \mu\text{m}$  and the hole size to separation ratio was approximately 0.35. This structure gave rise to a high nonlinearity and a zero dispersion point around 900 nm. The fiber therefore had a low and positive dispersion throughout the normal Ti:sapphire operating range (720 to 890 nm) and is therefore suitable for pulse compression across this range. For a longer operational input wavelength range, e.g., 900 to 1000 nm, a slightly different fiber with a longer wavelength zero-dispersion point would be required. The dispersion in the fiber used was estimated to be  $50 \text{ ps}/\text{nm km}$  at 800 nm.

Prior to the application of the PCF-assisted system for TPLSM, we quantified the operational properties of the fiber. A full description of the analysis is described elsewhere,<sup>10</sup> therefore here we present only the key outcomes. Figure 2(a) shows a typical transmission spectrum of the fiber output with 188 mW of light transmitted through 86 mm of fiber (representing a transmission of 61%). This corresponded to a pulse energy of  $\sim 2.35 \text{ nJ}$  at a laser wavelength of  $\lambda = 830 \text{ nm}$ . The spectrum shows the multipeak structure characteristic of self-

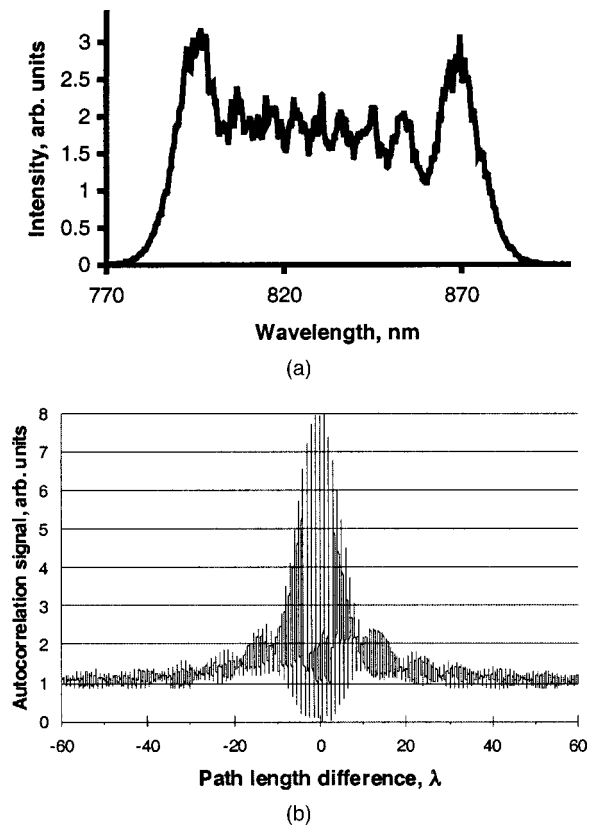


**Fig. 2** (a) Spectrum of the light transmitted through 86 mm of fiber at an average transmitted power of 188 mW. The spectrum shows a symmetric and approximately 38 THz wide distribution (FWHM) with nine individual maxima. (b) Experimentally recorded autocorrelation signal for an optimally compressed pulse at 175 mW transmitted power. The  $\sim 13.5$  fringes FWHM of this pulse correspond to a compressed pulse width of 25 fs. The dispersion required for optimum compression prior to entering the scan head is  $1.22 \times 10^{-3} \text{ ps}^2$ .

phase modulation with a broadening to 40 THz. Additionally, the spectral bandwidth was observed to increase linearly with the power transmitted through the fiber. The combined effect of the nonlinear self-phase modulation and the positive dispersion in the PCF was an almost linear frequency variation across the pulse (chirp). This linear variation enabled the use of the anomalous dispersion of a grating pair to compress the pulse.

To experimentally quantify the pulse shape from the fiber and grating pair we recorded the interferometric autocorrelation signal for the pulse, using a homemade collinear scanning autocorrelator based on two-photon absorption in a GaAsP photodiode.<sup>11</sup> Figure 2(b) shows an example of the recorded trace for 175 mW transmitted through the fiber at a wavelength of 830 nm. The initial grating separation was chosen to maximize the peak intensity or, equivalently, the autocorrelation signal. This was where we would expect the shortest pulses and hence the maximum two-photon response from the photodiode. The signal displayed the familiar symmetric shape with a peak to background ratio of 8:1. The notable difference compared with the familiar  $\text{sech}^2$  autocorrelation signal was the prominent structure in the wings due to side lobes on the pulse. The main part of the pulse is a narrow central feature containing 75% of the energy, while the re-

maining energy is distributed symmetrically in two sidelobes immediately adjacent to the central peak.

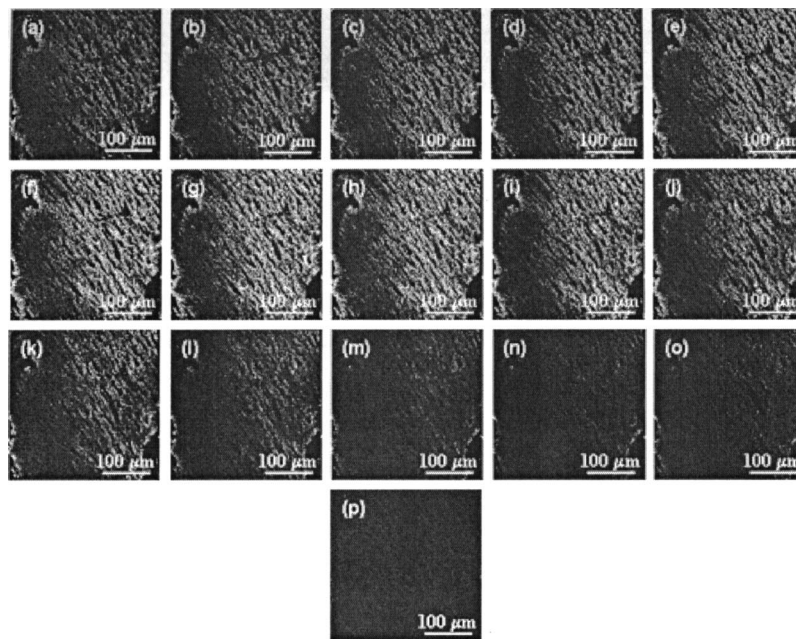
We calculated the ratio of the FWHM of a typical pulse and the number of interference fringes across the autocorrelation trace to be a constant 1.84 fs/fringe or slightly larger than the ratio of 1.44 fs/fringe for a  $\text{sech}^2$  pulse. The 13.5 fringes observed in the experimental data shown in Fig. 4 in Sec. 3 therefore correspond to a pulse width of 24.8 fs or an order of magnitude compression of the original laser pulse.

To demonstrate the benefits of the dispersion-compensated system, we performed TPLSM using both the PCF-enabled precompensation system and the commercial Ti:sapphire laser unit. The first sample imaged was guinea pig small intestine muscularis externa labeled with an antismooth muscle myosin primary antibody and Alexa 594-conjugated goat antimouse secondary antibody. To facilitate a complete comparison when used for direct two-photon excitation, the average power of the commercial source was set to 24 mW to exactly match that from the PCF-enabled system. Additionally, the output from the PCF-enabled system was manipulated to replicate the spatial characteristics of the commercial system to ensure identical filling of the objective lens. The imaging and capture system was identical in both configurations.

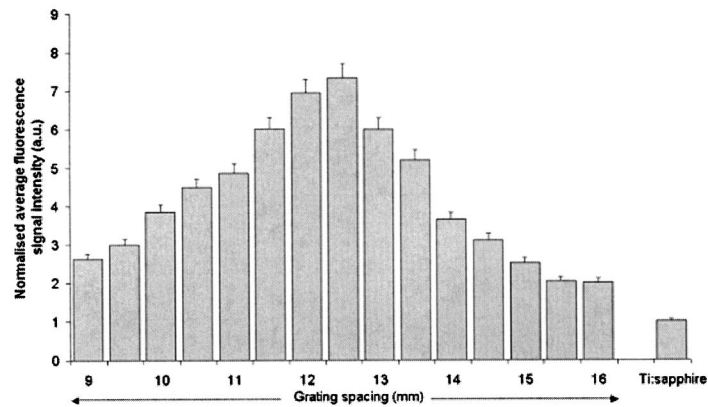
### 3 Results

Figure 3(a) to 3(o) shows a series of images taken with the PCF-enabled system when 24 mW of average power was delivered into the scan head, as configured in Fig. 2. The images were taken while changing the grating spacing from 9 to 16 mm and hence altering the effective pulse duration at the sample. For comparison, Fig. 3(p) shows the image obtained from applying the conventional Ti:sapphire laser at the same average power. The images were taken at a capture rate of  $\sim 1$  Hz, at  $256 \times 256$  pixels box size. The repetition rate, average power and spatial beam properties of both the PCF-assisted and the conventional Ti:sapphire laser systems were identical: the only difference was the pulse duration and hence the peak intensity of the radiation reaching the sample.

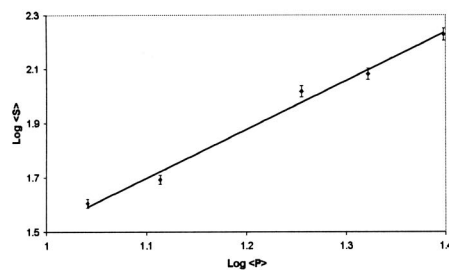
In comparison with the conventional excitation source, a more than sevenfold increase in fluorescence yield was consistently obtained under two-photon excitation of the sample with the PCF-enabled system. This is shown in Fig. 3(q), where a 7.3 times increase in fluorescence signal intensity was measured using image analysis software (LaserPix, Bio-Rad) when switching from the conventional Ti:sapphire laser source to the PCF-assisted laser for the sample described in Figs. 3(a) to 3(o). These data are taken from a sample of  $n = 10$  and are normalized with respect to the fluorescence yield from conventional Ti:sapphire excitation. From this, we inferred that the pulse duration at the sample was more than a factor of seven times shorter using the PCF-enabled system. We therefore calculated a pulse duration of  $< 35$  fs arriving at the sample. This was more than an order of magnitude shorter than was previously measured using another commercial TPLSM system.<sup>12</sup> By attenuating the PCF-assisted source, a near-quadratic relationship (gradient of  $1.8 \pm 0.1$ ,  $n = 20$ ) between the average fluorescence signal intensity and increasing average laser power was observed at a grating spacing of 12 mm, as shown in Fig. 3(r). This confirmed the nonlinear nature of the excitation mechanism.



(a)



(b)



(c)

**Fig. 3** (a) to (p) Series of TPLSM images of guinea pig small intestine muscularis externa labeled with antismooth muscle myosin an Alexa 594-conjugated antibody for smooth muscle myosin, using both the PCF-enabled system (a) to (o) and the commercial Ti:sapphire laser unit (p). The grating spacing of the PCF-enabled system was increased from (a) to (o) 16 mm in 0.5-mm increments, and hence changed the effective pulse duration at the sample. (q) Fluorescence yield from PCF-enhanced and conventional Ti:sapphire two-photon excitation of guinea pig small intestine muscularis externa labeled with antismooth muscle myosin and Alexa 594. A 7.3 times increase in fluorescence signal intensity was measured. (r) By attenuating the PCF-assisted source, a near-quadratic relationship (gradient of  $1.8 \pm 0.1$ ,  $n = 20$ ) between average fluorescence signal intensity and increasing average laser power was observed while imaging guinea pig small intestine muscularis externa labeled with antismooth muscle myosin and Alexa 594. This confirmed the nonlinear nature of the excitation mechanism.

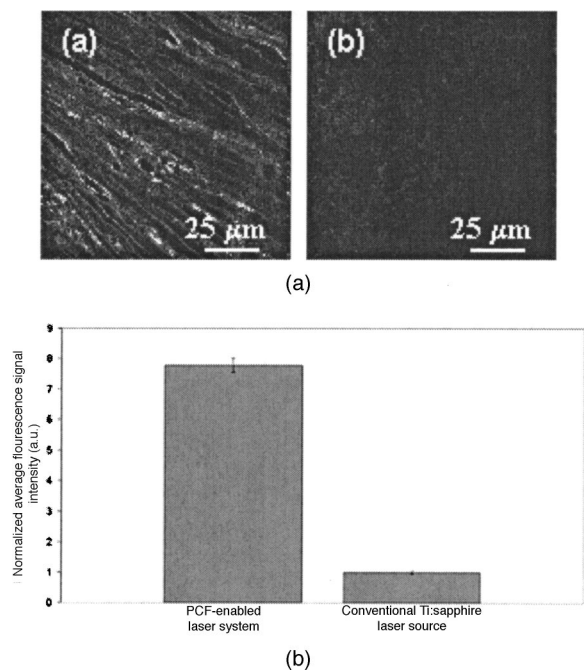


**Fig. 4** (a) and (b) Smooth muscle cells in intact, living rat pulmonary artery, labeled with the voltage sensitive dye di-8-ANEPPS were imaged using TPLSM. With an average power of 22 mW from both systems directed into the scanhead, (a) shows the image obtained with the PCF-enabled source at a grating spacing of 14 mm, while (b) depicts the image generated using the conventional Ti:sapphire laser. (c) Fluorescence yield from PCF-enhanced and conventional Ti:sapphire TPLSM of intact, living rat pulmonary artery, labeled with the voltage sensitive dye di-8-ANEPPS. A 7.8 times increase in fluorescence signal intensity was routinely observed.

This grating separation was somewhat larger than the few mm found to be optimal for the direct pulse measurements.<sup>10</sup> We attribute this to the positive dispersion of the microscope system, which is effectively being precompensated by an increased negative dispersion from the grating pair. The fact that we do not observe a full 10-fold increase in the signal that might be anticipated from the order of magnitude reduction in the pulse width most probably results from the increased higher order dispersion of the optical system, which is not compensated in the present implementation.

Similar experiments comparing the PCF-enhanced system with the normal Ti:sapphire laser by imaging smooth muscle cells in intact, living rat pulmonary artery, labeled with the voltage sensitive dye di-8-ANEPPS were also performed. The images were taken at a capture rate of ~1 Hz, at a 256- $\times$ 256-pixel box size, using a 60 $\times$ /1.4 NA oil microscope objective lens (Nikon). The repetition rate, average power, and spatial beam properties of both the PCF-assisted and the conventional Ti:sapphire laser systems were identical; again, the only difference was the pulse duration of the radiation reaching the sample. With an average power of 22 mW from both systems directed into the scan head. Figures 4(a) and 4(b) show the images obtained with the PCF-enabled source [Fig. 4(a)] and the conventional Ti:sapphire laser [Fig. 4(b)] at a grating spacing of 14 mm. This 2-mm increase in grating spacing from the previous investigation of guinea pig small intestine muscularis externa compensated for the positive dis-

persion arising from the immersion oil and the alternative microscope objective lens used. Application of the PCF-enabled laser source resulted in a 7.8-fold enhancement of fluorescence intensity when compared with direct excitation from the commercial Ti:sapphire laser. This is shown in Fig. 4(c). The TPLSM imaging process did not observably compromise either of the samples investigated, although previous reports indicate that the probability of cell destruction through TPLSM increases with a decrease in pulse duration.<sup>13</sup>

Over a typical imaging period of 9 h, no alignment of the PCF or associated beam-steering optics was required to maintain a >sevenfold enhancement of fluorescence intensity compared with conventional excitation. Additionally, no short-term instability was observed during image capture at a rate of 1 Hz.

These results demonstrate the considerable potential of the PCF-augmented system as a practical addition to markedly improve existing MPLSM systems for both fixed and live sample imaging. This is of particular importance in the instance of samples with weakly responsive fluorophores or those with only a small overlap of absorption wavelength with the emitting wavelength of the exciting USP laser source. Additionally, the increase in peak power due to the reduction in pulse duration indicates that the average power of the laser source can be decreased. This should improve sample integrity through reduced linear absorption of the excitation source.

#### 4 Discussion

Although we realized more than a sevenfold increase in fluorescence yield, it should be possible to increase this further by optimizing the pulse compression conditions of the PCF, based on a fixed USP laser. The optimum condition for pulse compression based on standard, single-mode step-index fibers was determined theoretically by Tomlinson et al.<sup>9</sup> and applies equally well to the PCF system. The optimum compression factor  $F_c$  was found to have the following dependence on input parameters:

$$F_c \propto T_0 \left( \frac{I_0}{|\beta_2|} \right)^{1/2}, \quad (1)$$

where  $I_0$  is the peak intensity in the pulse,  $T_0$  is the input pulse duration, and  $\beta_2$  is the group velocity dispersion. This expression immediately shows the advantage of using a PCF. The small fiber cross section compared with conventional optical fiber leads to a high peak intensity and the PFC provides the freedom to choose a suitably low GVD for the particular wavelength region of interest. Applying relevant experimental fiber parameters to the detailed theory we found a maximum compression factor of 35, which would be obtained<sup>10</sup> at a fiber length of 40 cm. We were forced to use an approximately five times shorter than optimal length of fiber, as the bandwidth of the pulse would otherwise have extended into the anomalously dispersive regime. The observed compression factor is therefore in reasonable qualitative agreement with this theory.

As mentioned, the high compression factor obtainable with a PCF is partly due to the relatively small GVD. This, in turn, is at least partly due to the laser operating near the zero point for the dispersion. In our experiments, this was too close for

the required bandwidth for an optimally compressed pulse. However, the dispersive properties of PCFs can to some extent be tailored<sup>6,7</sup> offering the enticing prospect of designing a fiber structure optimized for pulse compression. The fiber would have a small and highly nonlinear core and a relatively small, positive, and as near as possible constant GVD over a bandwidth of a few hundred nanometers.<sup>14</sup> This would enable the same piece of fiber to be used over a wide wavelength range. We will experimentally investigate this optimization process in due course.

## 5 Conclusion

We demonstrated the use of PCF in combination with a grating pair for pulse compression of 250-fs Ti:sapphire laser pulses to below 25 fs, and the subsequent improvement in TPLSM when applying conventional commercial systems. More than a sevenfold increase in fluorescence intensity yield was routinely measured using simple image analysis methods. From this we deduce a factor of 7 reduction in the pulse duration reaching the sample to <35 fs. We also investigated the ideal parameters for optimum pulse compression, and we anticipate that pulses less than 10 fs at the sample can be achieved using this technique. The experimental configuration was very basic, requiring comparable optomechanical precision with commercial imaging solutions, yet offered an unrivaled increase in fluorescence enhancement.

## Acknowledgments

This work was carried out in collaboration with NKT Research and Innovation A/S and Crystal Fiber A/S, from whom the fibers were obtained. The authors acknowledge Ross Davidson, Karen McCloskey, and Alison Gurney for supplying and preparing the samples used in this investigation.

## References

1. W. Denk, J. H. Strickler, and W. W. Webb, "Two-photon laser scanning fluorescence microscope," *Science* **248**, 73–76 (1990).
2. A. Diaspro and M. Robello, "Two-photon excitation of fluorescence for three-dimensional optical imaging of biological structures," *Photochem. Photobiol.* **55**, 1–8 (2000).
3. M. Müller, J. Squier, R. Wolleschensky, U. Simon, and G. J. Brakenhoff, "Dispersion precompensation of 15 femtosecond optical pulses for high-numerical-aperture objectives," *J. Microsc.* **191**, 141–150 (1998).
4. D. G. Ouzounov, K. D. Moll, M. A. Foster, W. R. Zipfel, W. W. Webb, and A. L. Gaeta, "Delivery of nanjoule femtosecond pulses through large-core microstructured fibers," *Opt. Lett.* **27**, 1513–1515 (2002).
5. J. C. Knight, T. A. Birks, P. St. J. Russell, and D. M. Atkin, "All-silica single-mode optical fiber with photonic crystal cladding," *Opt. Lett.* **21**, 1547–1549 (1996).
6. T. A. Birks, J. C. Knight, and P. St. J. Russell, "Endlessly single-mode photonic crystal fiber," *Opt. Lett.* **22**, 961–963 (1997).
7. J. K. Ranka, R. S. Windeler, and A. J. Stentz, "Visible continuum generation in air silica microstructure optical fibers with anomalous dispersion at 800 nm," *Opt. Lett.* **25**, 25–27 (2000).
8. A. V. Husakou and J. Hermann, "Supercontinuum generation of higher-order solitons by fission in photonic crystal fibers," *Phys. Rev. Lett.* **87**, 203901–203904 (2001).
9. W. J. Tomlinson, R. H. Stolen, and C. V. Shank, "Compression of optical pulses chirped by self-phase modulation in fibers," *J. Opt. Soc. Am. B* **1**, 139–149 (1984).
10. G. McConnell and E. Riis, "Ultra-short pulse compression using photonic crystal fibre," *Appl. Phys. B* (in press).
11. J. K. Ranka, A. L. Gaeta, A. Baltuska, M. S. Pshenichnikov, and D. A. Wiersma, "Autocorrelation measurement of 6-fs pulses based on the two-photon-induced photocurrent in a GaAsP photodiode," *Opt. Lett.* **22**, 1344–1346 (1997).
12. D. Wokosin, Private Communication.
13. K. König, T. W. Becker, P. Fischer, I. Riemann, and K.-J. Halhuber, "Pulse-length dependence of cellular response to intense near-infrared laser pulses in multiphoton microscopes," *Opt. Lett.* **24**, 113–115 (1999).
14. A. Ferrando, E. Silvestra, J. J. Miret, and P. Andrés, "Nearly zero ultraflattened dispersion in photonic crystal fibers," *Opt. Lett.* **25**, 790–792 (2000).